Global transcriptional regulators fine-tune the translational and metabolic machinery in *Escherichia coli* under anaerobic fermentation

Mahesh S. Iyer[1, #], Ankita Pal[1, #], Sumana Srinivasan[1], Pramod R. Somvanshi[1], K.V. Venkatesh[1, *]
[1]Department of Chemical Engineering, Indian Institute of Technology Bombay, Powai, Mumbai-400076, India.
[#]Co-first author
[*]Corresponding author

Abstract

Complex regulatory interactions between genetic and metabolic networks together confer robustness against external and internal perturbations in an organism such as *Escherichia coli*. This robustness comprises of cost-effective metabolism contemplating the benefit in resource investment coordinated by the interplay between growth-rate dependent machinery and global transcriptional regulators. Here, we reappraise the role of global transcriptional regulators FNR, ArcA and IHF fundamental for optimal growth of *E. coli*, under energetically less favourable albeit proteome-efficient anaerobic fermentative conditions. We reveal at the transcriptome and metabolome level, that absence of these global regulators ensued a disruption of nitrogen homeostasis, overexpression of otherwise unnecessary or hedging genes and impairment in core bottleneck steps and amino acid metabolism. Notably, our findings emphasize their importance in optimizing the metabolic proteome resources essential for rapid growth. Consequentially, the perturbations in the metabolic proteome as a result of deletion of global regulators unbalances the ribosomal proteome share imposing a high translation program at the expense of lowered efficiency. We illustrate that disruption of this inherent trade-off between metabolic and ribosomal proteomic investment eventually culminate to lowered growth rate. Despite no changes in gene expression related to reduced glucose import, our findings elucidate that the changes in intracellular metabolites directly modulated by growth rate, in turn feedback regulates the glucose uptake. Our results employing the proteome

allocation theory and quantitative experimental measurements, suffices to explain the physiological consequences of altered translational and metabolic efficiency in the cell, driven by the loss of these global regulators.

Introduction

In gram-negative bacteria, *Escherichia coli*, due to the huge expenditure associated with protein synthesis especially ribosomes, a tight coordination of the proteomic resources with the metabolic needs is fundamental for cell proliferation (1–3). Such investments need to be carefully tailored to specific environmental conditions, including the energetically least favourable anaerobic fermentation that harbours a lower proteome cost for energy production *per se* (4). This entails bacterial growth to be precisely controlled by the joint effect of global physiological factors (e.g. RNA polymerase, ribosome, metabolites) and transcriptional regulators (5, 6).

The global transcriptional regulators, FNR (Fumarate and Nitrate Reductase), ArcA (Aerobic respiration control A) and IHF (Integration host factor) occupies the top-most hierarchy of transcriptional regulatory network (TRN) based explicitly on the number of genes they regulate (7). Genome-wide binding studies for global regulators like FNR and ArcA in varied oxygenation and nutritional conditions are well appreciated (8–12). Conventionally, broad overview of the role of these regulators in sensing metabolic redox state, influence of oxygen on their activity and the regulatory networks governing central carbon metabolic responses have been thoroughly investigated using gene expression, mutational studies and metabolic flux analyses in anaerobic and micro-aerobic environments (9-20). Similarly, IHF has been well-characterized as a nucleoid protein and for its regulatory effects under diverse nutritional conditions (21–26) . However, studies enumerating the significance of FNR, ArcA and IHF in orchestrating metabolism and protein economy favouring growth fitness in anaerobic fermentation of glucose is yet to be uncovered. Therefore, a detailed investigation of the causality of regulator deletion on transcriptome of the organism in response to anoxic

conditions will deepen our understanding of how the organism behaves with shifts in its optimality. Further, studies that address their regulatory control on nitrogen and sulphur sensing mechanisms apart from carbon are limited. Thus, revisiting such global regulatory mechanisms not only at the transcript level but also the metabolome and proteome level, will shed light on quantitative cellular responses to internal or environmental cues.

Here, we elaborate that disruption of FNR, ArcA and IHF affects the allocation of global cellular factors (e.g. RNA polymerase, ribosome, metabolites) and causes imbalanced proteome allocation that governs the optimality of the organism, using a systems biology approach (transcriptomics, ^{13}C-metabolomics and phenomics). We first characterized the transcriptomic responses under glucose fermentative conditions that helped us to identify known and novel signature genes specific to the regulators which overall represented dysregulation of common metabolic pathways. We demonstrated that all these regulators exhibit control over nitrogen sensing mechanism, repress unnecessary genes under anaerobic fermentation and impact the biosynthesis and bottleneck reactions in central metabolic pathway. Collectively, they represent the core metabolic proteome essential for rapid growth and their impairment directly influences the metabolome of the organism. Further, we validated our findings using a simple quantitative model (27–30) that revealed an alteration in translational and metabolic efficiency as a function of the disruption of proteome allocation, attributed to the loss of regulators. Overall, our work suggests that these global regulators fine-tune the metabolic and translational machinery, thereby ensuring sector-specific proteome distribution, conducive for balanced growth. Such studies can elucidate the general design principles underlying the importance of global regulators in *E. coli*, that spans more than 30 years of research.

Results

Disparate transcriptome profiles of global regulator mutants converge to a common phenomenon of metabolic impairment

First, to address the transcriptomic changes caused by the disruption of global regulators namely FNR, ArcA and IHF in *E. coli* K12 MG1655 under anaerobic glucose fermentative condition, we performed a high coverage RNA-seq from the samples harvested in the mid-exponential phase. Preliminary analysis of RNA-Seq data revealed a total of ~314, ~258 and ~580 differentially expressed genes (DEGs) in Δ*fnr*, Δ*arcA* and Δ*ihf* mutants respectively, compared to the wild-type strain (WT) (Figure S1). The Δ*fnr* and Δ*arcA* mutant showed a distinct pattern in its DEGs, wherein we observed higher number of downregulated genes (~66%) in Δ*fnr* mutant and higher number of upregulated genes (~67%) in Δ*arcA* mutant. This result reiterated their predominant role as transcriptional activator and repressor, respectively (10–12,19). On the contrary, in Δ*ihf* mutant, the number of upregulated (53%) and downregulated (47%) genes were comparable with slightly higher median fold-change (FC) in case of downregulated genes ($P < 0.05$, Mann Whitney test).

We compared our gene expression data with previous studies and consistently found a lower yet significant percentage of DEGs directly regulated by FNR, ArcA and IHF respectively (Figure S2). Moreover, DEGs also showed enrichment for RNA polymerase with either stress-related sigma factor, sigma 38 or nitrogen-related factor, sigma 54 apart from the growth associated sigma factor 70 (Figure S2). This reflected a sub-optimal allocation of growth-rate dependent global machinery as an indirect consequence of loss of these regulators.

Further, we enriched the DEGs for each of the mutants using KEGG pathway hierarchical classification to understand the role of these regulators on key metabolic pathways (Figure S3-S5). We observed a common enrichment (adj-P value < 0.05) of pathways such as Amino acid metabolism and Transport related pathways across all the mutants. Additionally, we observed

enrichment of pathways pertaining to TCA cycle and anaplerosis and alternate carbon metabolism (e.g. lipid and steroid metabolism, glycerol or secondary carbon degradation) in these mutants. Altogether, such enrichments underscore the metabolic impairment prevalent as a result of loss of these global regulators.

Perturbation in nitrogen homeostasis

We investigated the gene-level changes associated with the enrichment of Amino acid metabolism and Transport related pathways in all the mutants (Figure 1). Specifically, we observed upregulation of putrescine (*puuABCE*) and arginine degradation (*astABCDE*) genes in Δ*fnr* and Δ*arcA* mutants. These genes belong to pathways that yield glutamate and ammonia as end products and can independently satisfy *E. coli*'s nitrogen requirement (31, 32). Perhaps, upregulation of these genes indicated a scavenging mechanism to restore possible disruption of the nitrogen balance in the cell. In addition, we observed downregulation of ATP-dependent organic nitrogen transporters namely arginine (*artIJ*) and methionine (*metN*) transporters in Δ*arcA*, and glutamine (*glnHP*) and leucine/phenylalanine (*livHKM*) transporters in Δ*fnr*. These gene responses indicated an impairment in amino acids or nitrogen sources import, as a common trend among these mutants.

Similar observation of nitrogen limitation was prevalent in Δ*ihf* (Figure 1). For instance, upregulated genes enriched for Transporters in Δ*ihf*, code for efflux of polyamines like putrescine (*sapABCDF*) and spermidine (*potC, mdtIJ*), which represent organic nitrogen reservoirs, known to be involved in protein synthesis contributing to cell proliferation (33). Under nitrogen replete conditions, *E. coli* resorts to increasing gene expression of ATP-dependent nitrogen uptake and two-component nitrogen sensing systems, sufficient enough to sustain cell growth (34). Consistent with this, we observed upregulation of *amtB and glnKLG* genes in Δ*ihf*. In addition, we observed upregulation of amino acid biosynthesis genes such as glutamine (*glnA*) and tryptophan (*trpACDE*) in Δ*ihf*. This phenomenon was in agreement with

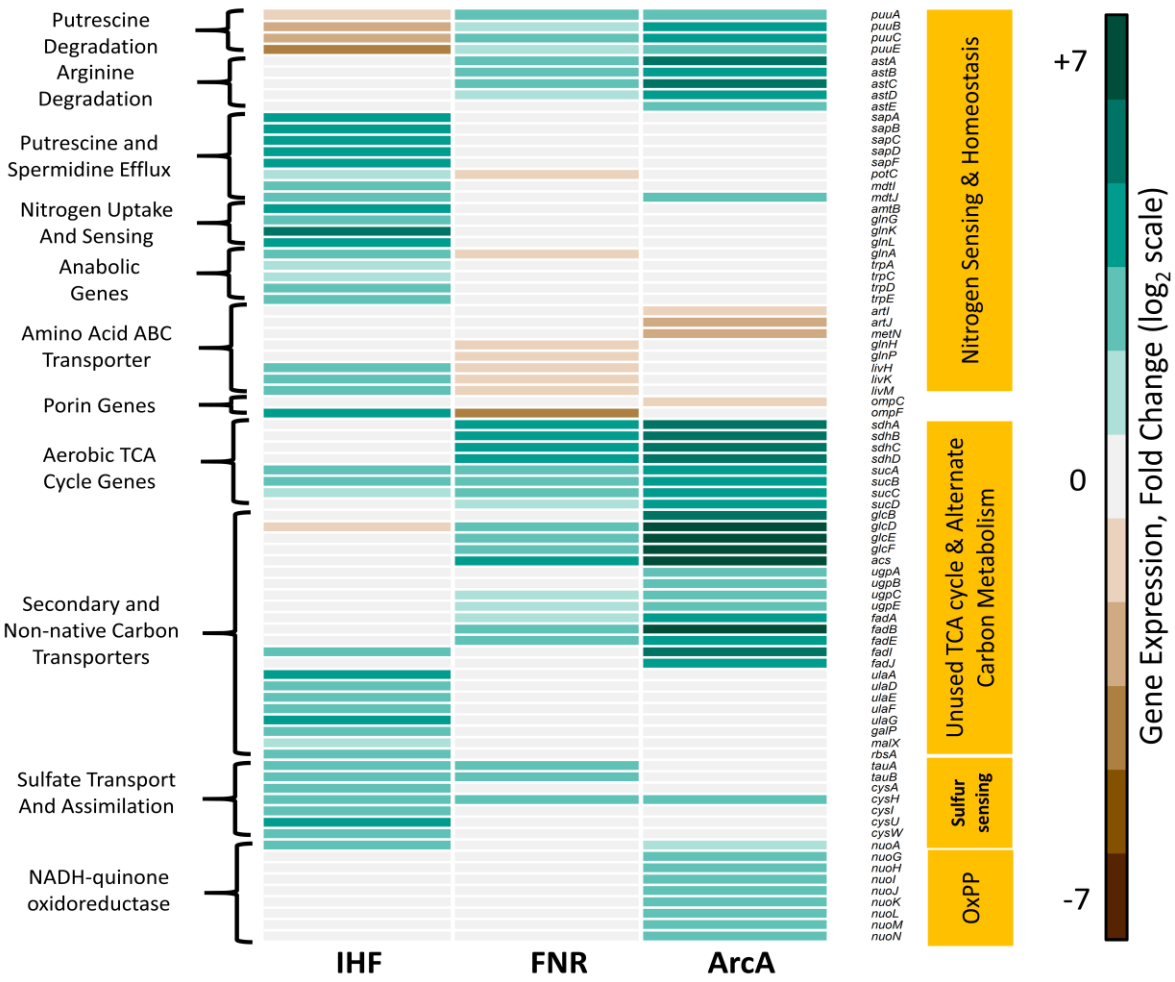

Figure 1: Heatmap of representative DEGs in Δ*ihf*, Δ*fnr* and Δ*arcA* strains, each compared to WT. The figure shows specific genes enriched by KEGG pathway classification (shown in Supplementary Figure S3-S5) that were functionally categorised using evidences from Ecocyc database. Broadly, loss of these global transcriptional regulators were found to commonly affect genes involved in nitrogen sensing and homeostasis, unused TCA cycle and alternate carbon metabolism, sulphur sensing and oxidative phosphorylation (OxPP). Gene expression values are obtained from average of two biological replicates (n=2) expressed as log2 Fold change. The downregulated genes are shown in brown and the upregulated genes are shown in cyan.

the previous observation wherein, anabolic genes showed increased expression in response to nitrogen limitation (29).

Moreover, we observed downregulation of porin genes, *ompC* and *ompF* in Δ*arcA* and Δ*fnr* respectively, and upregulation of *ompF* in Δ*ihf* mutants (Figure 1). Again, alteration of these porin genes conform to the defect in nitrogen transport apart from reflecting the osmotic imbalance in the cell (35). Overall, the perturbation in amino acid metabolism and transport elucidated the novel role of these global regulators in regulating the nitrogen homeostasis and sensing mechanism in *E. coli*.

De-repression of genes unnecessary in anaerobic fermentation

Our analysis indicated an upregulation of TCA cycle and anaplerosis pathway in Δ*fnr* and Δ*arcA* (Figure S4-5) that involved genes coding for the aerobic respiratory TCA cycle, consistent with previous data (10-12,16). Apart from being unnecessary under the anaerobic fermentative conditions, these genes also incur a substantial protein synthesis cost (36). In addition, we observed a significant upregulation of alternate carbon metabolism genes such as glycolate degradation (*glcBDEF*), glycerol degradation (*ugpABCE*) and acetate uptake (*acs*) in Δ*fnr* and Δ*arcA* (Figure 1). This represents a hedging mechanism wherein a bacterial cell when challenged with fluctuating or unfavorable environmental conditions, modulates its gene expression so as to prepare themselves conducive to alternate metabolic phenotypes (37, 38). Furthermore, our DEGs showed significant upregulation of aerobic oxidative phosphorylation (*nuoAGHIJKLMN*) and unused lipid and steroid metabolism (*fadABEIJ*) related pathways in Δ*arcA*.

Similarly, Δ*ihf* showed significant upregulation of alternate carbon metabolism genes responsible for ascorbate (*ulaADEFG*), galactose/maltose (*galP*, *malX*), and ribose (*rbsA*) catabolism (Figure 1). We further revealed upregulation of genes coding for transporters of sulfur sources (*tauAB* and *cysAUW*) as well as sulphate assimilation (*cysHI)*, as a common response to sulfur limitation prevalent in Δ*ihf*. Overall, the upregulation of genes pertaining to unused or hedging proteins under conditions of anaerobic fermentation, can impose a burden on the growth of the organism.

Regulatory control on amino acid biosynthesis and bottleneck steps in central carbon metabolic pathway

In order to effectively examine the control on amino acid biosynthesis and specific bottleneck reactions pertaining to central carbon metabolism, we monitored the absolute intracellular concentration of metabolites in the mid-exponential phase using ^{13}C-based metabolomics coupled to its corresponding gene expression changes.

Among the precursor metabolites arising from glycolytic pathway, a pronounced effect was seen as an increased PEP accumulation in all the mutants (Figure 2 & S6). Presumably, this observation can be attributed to upregulation of *pck* in Δ*ihf* and Δ*arcA* and upregulation of *ppsA* and downregulation of *pykA* in Δ*fnr*, that have been reported to contribute to PEP synthesis during glycolysis (39). Also, we observed accumulation of branched chain amino acids derived from pyruvate, namely valine and leucine, in Δ*ihf* and Δ*fnr* mutant (Figure 2 & S6). This was in accordance with lowered gene expression of *ilv* observed for both the mutants, thereby indicating a negative feedback regulation of these amino acids on their biosynthesis. Additionally, in Δ*ihf*, we observed increase in levels of 3PG, a precursor for the amino acid glycine and serine, in concert with down-regulation of *gpmA* gene expression (Figure 2 & S7). However, only glycine levels were found to be higher in both Δ*ihf* and Δ*fnr*. Taken together, these results suggest that these regulators play a pivotal role in regulating glycolysis, majorly exerted through optimal metabolite levels of the pathway.

Next, we examined the TCA cycle intermediates such as α-ketoglutarate (αKG) and oxaloacetate (OAA) that are precursors for a large number of amino acids. It is well known that αKG that coordinates carbon and nitrogen balance by modulating glycolytic flux, accumulates during nitrogen limitation (40). Indeed, both Δ*ihf* and Δ*fnr* mutant showed accumulation of αKG in contrast to Δ*arcA* that showed a reduction (Figure 2 & S8). Additionally, the amino acids derived from αKG namely glutamate, proline and arginine, as

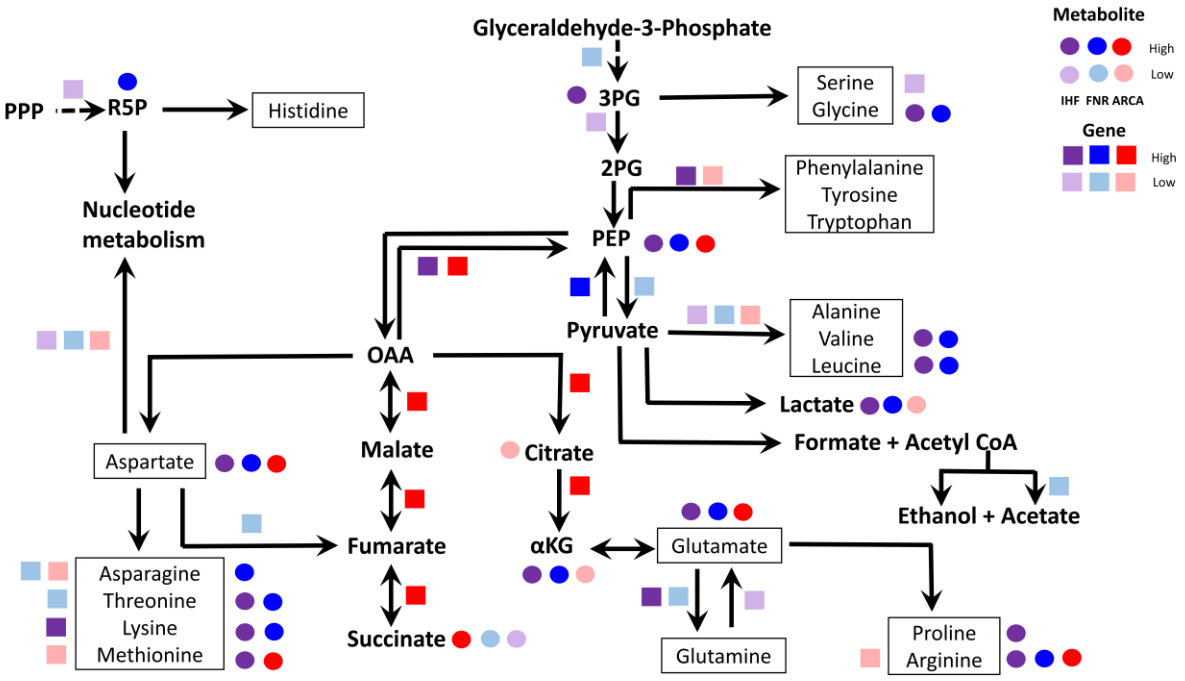

Figure 2: A schematic representation of the key steps in central carbon metabolic pathways affected by the deletion of the global regulators IHF, FNR and ArcA. The figure shows the unique pattern of regulatory control exerted on gene expression as well as metabolite levels. The genes are represented as coloured squares and metabolites are represented as coloured circles. Darker colour represents upregulation whereas light colours represent downregulation respectively. Only significant changes in gene expression and metabolite levels are depicted.

well as the amino acids derived from OAA namely aspartate, lysine, methionine and threonine were found to be significantly higher in Δ*ihf* and Δ*fnr* mutant (Figure 2 & S9). In Δ*arcA*, concomitant with increase in glutamate and aspartate levels, we observed increased accumulation of arginine and methionine respectively that were in line with down-regulation of methionine and arginine biosynthesis genes, reiterating feedback repression (Figure 2 & S8-9). Hence, in accordance with reduction in expression of amino acid biosynthesis genes and osmotic stress ensued in the absence of regulators, such accumulation indicated the inability of the organism to efficiently utilize the amino acids towards protein biomass essential for optimal growth.

Noteworthy, our data indicates the downregulation of nucleotide biosynthesis (derived from aspartate) in all the mutants, which succinctly explains the regulatory control on purine and pyrimidine metabolism (Figure 2 & S7). Concomitant with increase in aspartate levels, we

observed an increase in NAD levels in Δ*ihf* and Δ*fnr*, although *pntAB* gene involved in NAD dephosphorylation was downregulated solely in Δ*fnr* (Figure S7). Additionally, we predict a higher redox state (NADH/NAD ratio) in Δ*arcA*, as inferred from lower level of NAD along with increase in gene expression of NAD phosphorylating *sthA* and decrease in non-proton translocating NADH dehydrogenase *ndh* (Figure S5A), a phenomenon consistent with previous studies (12). To summarize, we observed direct and indirect effect on the metabolome due to the absence of global regulators, that corroborated with the upset in gene expressions in amino acid biosynthesis and other bottleneck reactions.

Physiological characterization highlights the growth sub-optimality

Severe perturbation in metabolic processes due to regulator deletion, motivated us to examine their physiological effects on the organism. Characterization of the phenotype of the mutants revealed a reduction of ~16-25% ($P < 0.05$, Students t-test) in growth rate as well as glucose uptake rate compared to WT (Table S1). The decrease in growth rate was found to be positively correlated with decrease in glucose uptake rate (Pearson correlation coefficient (PCC) ~ 0.98, $P < 10^{-3}$, Figure S10). Although glucose uptake rates were significantly lowered ($P < 0.05$, Student's t-test), the *ptsG* gene that is solely responsible for glucose uptake was not differentially expressed in any of the mutants. Nevertheless, the decrease in glucose uptake was in agreement with the accumulation of PEP observed across the mutants (PCC ~ -0.9, $P < 0.05$, Figure S10). We, further measured fermentation products or exo-metabolites namely formate, acetate, ethanol, lactate, succinate and pyruvate arising from anaerobic fermentation and calculated the yields by normalizing their absolute secretion rates to their respective glucose uptake rates (Table S1). Succinate yield was found to vary among the mutants, wherein, Δ*fnr* showed ~55% decrease and Δ*arcA* showed ~33% increase, in comparison to WT (Figure 2). Anaerobic succinate formation (32), involves two steps, wherein 1) aspartate to fumarate formation is catalyzed by *aspA* and 2) fumarate to succinate formation is catalyzed by *frd* genes

coupled to NADH cycling *nuo* genes. Hence, changes in succinate yield can be attributed to the reduction in gene expression of *aspA* in case of Δ*fnr* and upregulation of *nuo* genes in Δ*arcA* (Figure S9 & S5B). Our findings were consistent with previous studies reporting increased succinate yields in Δ*arcA* and reduced succinate yields in Δ*fnr* (10–12, 16). Additionally, we obtained higher lactate yield in Δ*fnr*, that had strong correlations (PCC ~ 0.95, $P < 0.005$) with branched chain amino acids namely leucine and valine, both being derivatives of pyruvate (Figure S10). Next, we measured the rate of ammonia uptake as an indicator of the nitrogen status of the organism. All the mutants showed a reduced ammonia uptake rate ($P < 0.05$, Student's t-test) compared to the WT (Table S1) reflecting the nitrogen limitation faced by the organism, congruent with our gene expression and metabolite data (αKG, arginine, glutamate) as well. Thus, our data showed a profound effect on growth physiology, glucose and nitrogen import, thereby elaborating the system-wide effect of deletion of global regulators (Figure 2).

Global regulators control the translation and metabolic efficiency of the organism

To explain the underlying mechanism as to how perturbations in core metabolic genes due to the loss of regulator resulted in reduction in growth rate and subsequent glucose uptake, we recalled a proteome allocation model that quantitatively relates the cellular ribosome content to the growth of *E. coli* (27–30). As explicitly outlined in the model (27), proteome sectors (∅) are comprised of: R-sector defining the growth-rate dependent ribosomal protein sector, M-sector defining the metabolic protein sector and Q-sector defining the growth-rate independent core proteome sector (Figure 3A). We defined an additional proteome sector "U", for the unused or unnecessary metabolic proteins, that help the organism hedge against altered environmental conditions but presumably poses a substantial proteomic burden under anaerobic fermentative conditions (Figure 3A). Based on the proteome conservation law empirically outlined in the model (27), all the aforementioned sectors add up to unity:

$$\emptyset R + \emptyset M + \emptyset U + \emptyset Q = 1 \quad (1)$$

wherein the maximal growth-related total proteome fraction comprises of sum of R-, M- and U-sectors other than $\emptyset Q$,

$$\emptyset_{max} = \emptyset R + \emptyset M + \emptyset U \quad (2)$$

Given,

$\emptyset_{max} = 1 - \emptyset Q$

The R-sector was derived from the product of experimentally measured RNA/protein (R/P) ratio 'r' with empirically derived conversion factor ρ = 0.76 (27) in each of the strains (Figure 3A). All the mutants in our study, showed a higher R/P value compared to the WT (Figure S11) with Δ*ihf* showing the highest R/P. We suggest that a higher R-sector might represent a compensatory countermeasure against the lowered growth of the mutants. Notably, previous study have experimentally validated the correlation of high ribosome content with lowered ppGpp levels (28). Interestingly, our analysis supports this notion in case of Δ*ihf* mutant, wherein genes that were reported to be positively regulated by ppGpp were downregulated ($P < 10^{-4}$, Fisher exact test), possibly suggesting a lowered level of ppGpp in this mutant. This observation also reiterated the previously deduced overlap in ppGpp and IHF targets (25). However, such enrichments were found to be insignificant in case of Δ*fnr* and Δ*arcA* mutants.

Increase in R-sector which incurs a huge proteomic cost (1, 2), reduces the available proteome resources towards M-sector thereby, indicating ribosomal proteins unnecessary in the mutants. Using the recently developed ME (for Metabolism and macromolecular Expression) model that accounts for 80% of *E. coli* proteome (41), we predicted the set of protein-coding genes belonging to M- and U-sectors as a function of growth rate (Supplementary file 4). First, we mapped the entire spectrum of DEGs in each of the mutants compared to WT to the ME model predicted protein-coding genes. Additionally, DEGs outside the scope of ME model were further enriched using KEGG pathway classification and added to M-sector and U-sector gene list based on manual annotation using Ecocyc (42, 43). We characterized the transcriptome

fractions of metabolic "M" sector and unnecessary/unused "U" sector (Supplementary file 4) using TPM (transcript per million) calculation as outlined in the methods section. Next, we calculated the unnecessary/metabolic (U/M) ratio based on these protein-coding transcriptome fractions, for each of the strains (Figure 3B). As expected, we observed a consistent increase in the U/M ratio across the mutants compared to WT, with the highest for Δ*fnr* followed by Δ*ihf* and Δ*arcA*. Finally, using the experimentally derived values of $\emptyset_{max}$ (~43%) reported previously (28, 29), R-sector proteome fraction and U/M ratio, we determined the M-sector proteome fraction as defined in Eq. (2).

For steady-state growth, the R-sector and M-sector proteome fraction have linear dependency on growth rate, described as:

$$\lambda = t_E \emptyset R \qquad (3)$$

$$\lambda = m_E \emptyset M \qquad (4)$$

where, phenomenological parameter t_E refers to translation efficiency (protein synthesis flux by R-sector proteome), phenomenological parameter m_E refers to metabolic efficiency (metabolic flux attained by M-sector proteome) and λ refers to the growth rate (h^{-1}) of the organism.

Further, by equating Eq. (3) and Eq. (4), we obtain the ratio of metabolic efficiency to the translation efficiency.

$$\frac{m_E}{t_E} = \frac{\emptyset R}{\emptyset M} \qquad (5)$$

Hence, using experimentally derived growth rates and R-sector proteome fraction, and empirically derived M-sector proteome fraction, we deduced the translational and metabolic efficiency in the mutants that quantifies the extent of regulatory defect (Figure 3C).

A

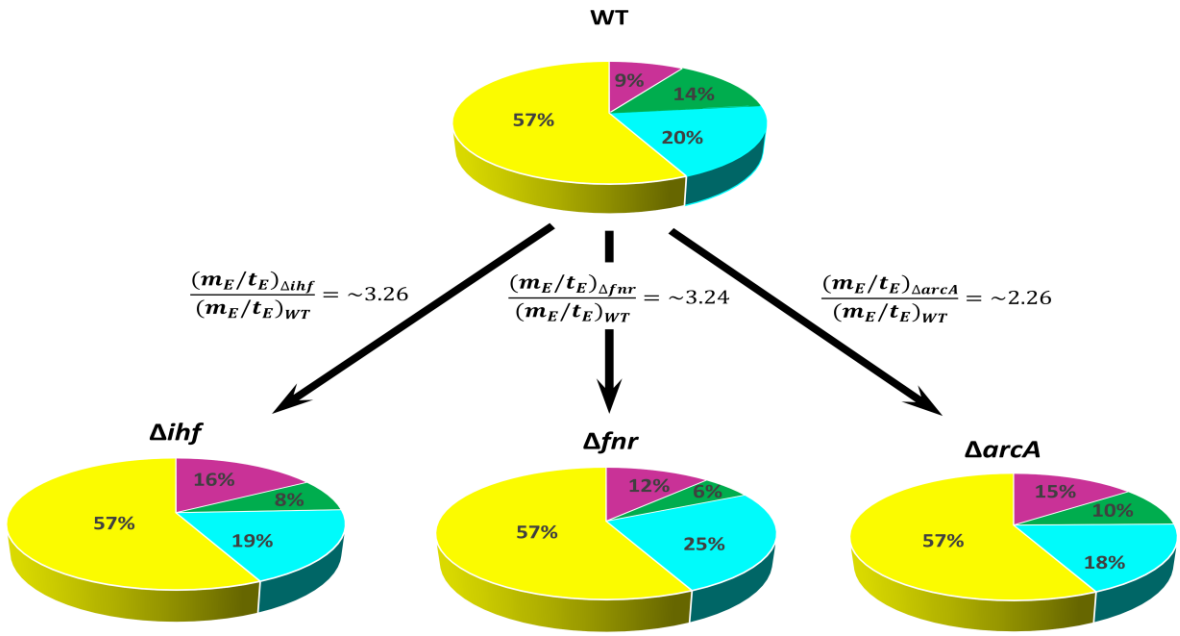

B

Mutants	U/M
WT	1.42 ± 0.07
Δ*ihf*	2.36 ± 0.3
Δ*fnr*	4.39 ± 0.38
Δ*arcA*	1.8 ± 0.05

C

Mutants	m_E/t_E
WT	0.64 ± 0.09
Δ*ihf*	2.07 ± 0.39
Δ*fnr*	2.06 ± 0.10
Δ*arcA*	1.44 ± 0.3

Figure 3. Proteome allocation in each of the strains. (A) A pie-chart depicting the quantitative distribution of the proteome sectors- R-sector, M-sector, Q-sector and U-sector as percentages, for the WT and the mutants. The figure indicates a high $\frac{m_E}{t_E}$ ratio in each mutant compared to WT. (B) The U/M protein-coding transcriptome fraction ratio for each of the strains. (C) The $\frac{m_E}{t_E}$ ratio derived for each of the strains.

Intriguingly, deletion of global regulators resulted in an increase in $\frac{m_E}{t_E}$ ratio, indicating a decrease in translation and increase in metabolic flux (Figure 3A-C). By normalizing the $\frac{m_E}{t_E}$ ratio for Δ*ihf*, Δ*fnr* and Δ*arcA* with WT ratio, we observed a concordant increase of ~3.26, ~3.24 and ~2.26 folds, respectively. The lowered t_E and high m_E as a result of imbalance in resource allocation, highlighted the inability of other growth-related physiological processes to counter the limitation due to the absence of global regulators (Figure 3A). Collectively,

employing the resource allocation model, we elucidated the role of the global regulators in precisely tuning the balance between translational and metabolic machinery that defines growth optimality.

Physiological consequences of altered m_E and t_E on glucose uptake rates

Next, we probed how steady-state metabolite accumulations subjected to changes in growth rate, might affect glucose uptake rates in each of the mutants. The amino acids and precursor pool-sizes can directly reflect the changes in t_E and m_E flux of the organism, given their linear association ($P < 0.05$, negative correlation, Figure S10A-C) with growth rate and glucose uptake rate in the mutants compared to WT (Figure S8). The accumulation of amino acids glutamate, aspartate and their derivatives observed consistently in the mutants (Figure S6-S9) owing to their inability to be incorporated into protein biomass, can be attributed to the reduction in t_E. Similarly, the increase in m_E was indicated by accumulation of precursors namely PEP, αKG, OAA (speculated from aspartate levels) in the mutants. In Δ*fnr* and Δ*ihf*, the intracellular concentration of αKG, when normalized to cell volume (2.3 µl/mg, (44), matches with its K_i (inhibition constant) value of 1.3 ± 0.1 mM for *ptsI* inhibition (40). *ptsI* codes for one of the components of the PTS system in *E. coli*, whose phosphorylation state determines the uptake rate of glucose. Thus, the higher intracellular concentration of αKG observed in Δ*fnr* and Δ*ihf* (Figure S8), can reduce the glucose uptake (PCC ~ -0.9, $P < 0.05$, Figure S10A-B) by non-competitive inhibition on the PTS (45). Similarly, OAA (speculated from aspartate levels, Figure S7), known to inhibit the glucose uptake (45), was found to be present at higher concentrations in all the three mutants, with Δ*arcA* having the highest aspartate accumulation (PCC ~ -0.9, $P < 0.05$, Figure S10C). Further, from the accumulation of leucine (PCC ~ -0.94, $P < 0.01$, Figure S10) and valine (PCC ~ -0.84, $P < 0.05$, Figure S10), increased lactate yield (PCC ~ -0.92, $P < 0.01$, Figure S10) and higher m_E (Figure 3C), we predict a high intracellular pyruvate pool in Δ*fnr*, that is known to adversely impact the glucose

import (45). Moreover, it is known that the intracellular accumulated carbon-rich amino acids such as aspartate, glutamate and glycine via their degradation to α-keto acids can affect the glucose uptake rate (Figure S10) (45). Further, reduction in glucose uptake in each of the mutants corroborated with the reduction in M-sector and increase in U-sector (Figure 3B), given that glucose import and processing in a minimal nutritional media involves significant metabolic proteome resources (4). Overall, global regulators FNR, ArcA and IHF, show a distinct control over amino acid metabolism, key metabolic bottleneck steps and unnecessary gene expression, thereby optimizing the translational and metabolic machinery conducive for balanced growth.

Discussion

In facultative anaerobe like *E. coli*, though anaerobic fermentation represents a less energetically favourable mode of metabolism, an efficient proteome allocation enables it to attain an economical phenotypic outcome (4). In this study, we elaborated an unexplored regulatory role of the global regulators FNR, ArcA & IHF, emphasizing their control over key metabolic processes fundamental for balanced physiological growth under anaerobic fermentation with glucose as a carbon source. Mechanistically, this work elucidated the "complimentary" role of these regulators with growth-rate dependent global machinery for optimal resource allocation.

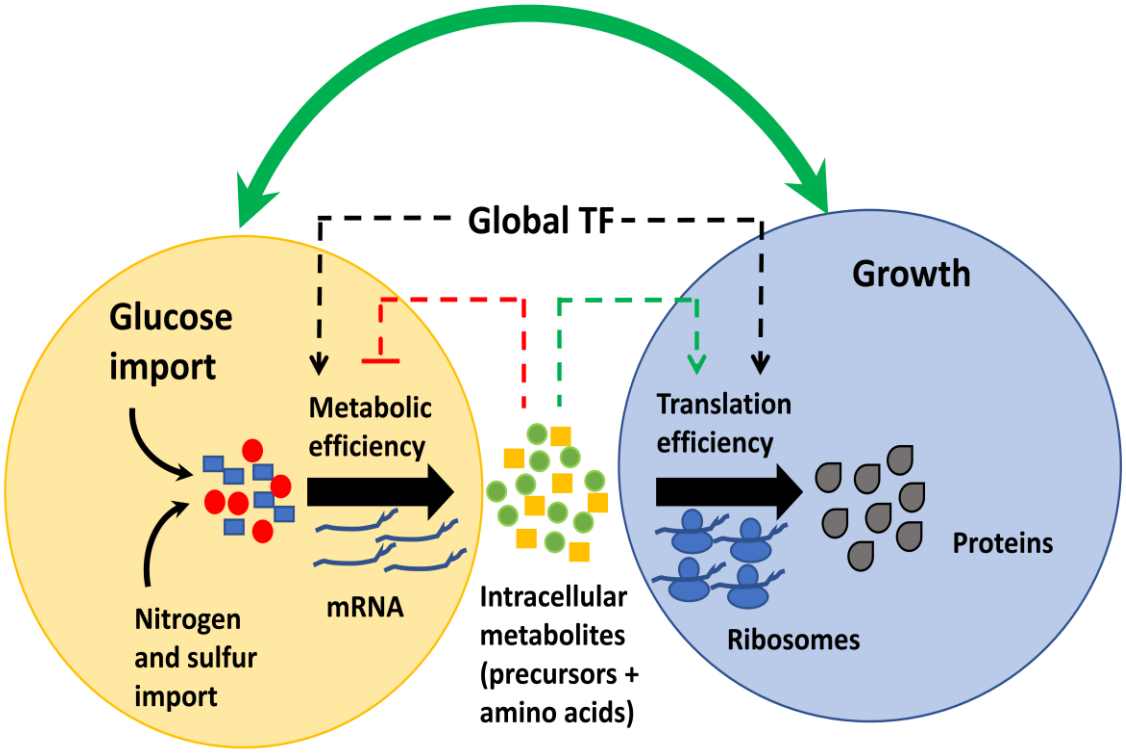

Figure 4. A model depicting global transcriptional regulator control on the metabolic and translational machinery. Carbon and nitrogen sources, following their uptake are processed into intracellular precursors and amino acids depending on the metabolic efficiency of the organism. These intracellular amino acids are then converted into proteins by ribosomes depending on the translation efficiency of the organism. The metabolic and translation efficiency of the organism is in turn feedback regulated by metabolites and genes under the purview of the regulators. Growth and glucose/carbon import have a strong linear association complemented by global regulators.

Our findings delineate the coordination between hierarchical (transcriptional regulators) and metabolite-driven regulation that direct the fueling products (e.g. precursors) and building blocks (e.g. amino acids) necessary for physiological growth (Figure 4). Transcriptionally regulating the first step or final committed step is sufficient enough to control the flux and end-product concentrations in the amino acid biosynthetic pathway, disruption of which entails osmotic imbalance (46,47). Perturbation observed in metabolite levels and gene expression of biosynthetic or bottleneck steps of central carbon metabolism explains this underlying regulation that modulate the glucose import and growth of the organism. Notably, we demonstrated that these global regulators control nitrogen homeostasis and sensing mechanism as evidenced from the induction of high-affinity nitrogen transporters or scavengers and from

the altered ammonia uptake. The present study quantitatively accounted for the reduction in metabolic proteins and increase in unnecessary or hedging proteins, when an optimal WT strain is debilitated by global transcription regulator deletion. This reduction in metabolic proteome directly impacts the phenotype, thereby imposing a high translation program reflected as high ribosomal proteome. However, owing to huge energetic cost associated with ribosomal synthesis itself, demand for increasing translation further constrains the proteome share for metabolic proteins. We illustrate that disruption of this inherent trade-off between metabolic and ribosomal proteomic investment involved a lower translational and higher metabolic efficiency, restraining growth. Nonetheless, the lowered t_E attempts to balance the perturbation in resource allocation by decreasing the synthesis of unnecessary and costly proteins although constraining the metabolic proteins as well. Concurrently, high m_E, attempts to balance the perturbation in resource allocation by increasing the carbon import and processing activity in response to general limitations of carbon. The changes in the phenomenological parameters t_E and m_E were manifested as accumulation of proteinogenic amino acids (glutamate, aspartate and their derivatives) and precursors (PEP, pyruvate, αKG & OAA), respectively. We identified a strong negative association of accumulating amino acids-precursors with glucose uptake and growth rate, reiterating the significance of metabolite control integral to metabolism. Since concentration of metabolites are critically controlled in the system and, given their feedback mechanisms directly impacting the t_E and m_E as depicted (Figure 4), any disturbance limits the potential of the system to attain growth rate as of WT. Overall, this addressed the interdependent association between growth rate and glucose uptake rate (green arrow in Figure 4), that feedback-regulate each other as per the demand and supply conferred on the system enabling fitter phenotype.

Under steady-state exponential growth conditions, protein levels are largely determined by their transcript concentrations albeit subjected to post-transcriptional or post-translational regulation (1). Literature survey suggests a modest correlation between mRNA and protein

levels, thus making it imperative to investigate the proteomic measurements together with metabolite interactions using mass spectrometry (48), to corroborate these results. Nevertheless, our approach addressed the general design principles comprising of the metabolic and translational flux ratio that would be less variant to such regulatory events. Also, given the myriad of factors that can convolute the regulatory and growth mediated effects, it would be imperative to address the transcription regulator by a titration-based approach obviating its pleiotropic effects and secondary effects of growth.

Collectively, we were able to demonstrate the indispensability of the regulators that exhibit control over key bottleneck steps, anabolic reactions, and genes associated with unneeded, stress or hedging metabolic proteins. Using a well-established yet simplified theory (27), we were able to comprehensively demonstrate that absence of these global regulators ensued an upset in necessary and unnecessary proteome homeostasis thereby resulting in sub-optimal translational and metabolic machinery. Broadly, such analysis can be extended to other global regulators like CRP (29, 49), HNS (50), Lrp (51) and Fis (52), which tempts us to anticipate similar underlying mechanisms of regulation, presumably not confined only to glucose metabolism.

DATA AVAILABILITY

The RNA sequencing data and the processed files from this study are available at NCBI Geo (https://www.ncbi.nlm.nih.gov/geo/query/acc.cgi?acc) under accession no. GSE153906. The metabolomics data presented in this study is available at the NIH Common Fund's National Metabolomics Data Repository (NMDR) website, the Metabolomics Workbench, https://www.metabolomicsworkbench.org where it has been assigned Project ID (PR000975). The data can be accessed directly via it's Project DOI: (10.21228/M8NX1G).

SUPPLEMENTARY DATA

Materials and methods, supplementary tables and figures are available in the Supplementary material.

FUNDING

This work was supported by DST fellowship/grant(SB/S3/CE/080/2015) and DBT fellowship/grant(BT/PF13713/BBE/117/83/2015) awarded to K.V.V., and DST-WOSA grant (grant number: SR/WOS-A/ET-58/2017) awarded to S.S.

ACKNOWLEDGEMENTS

We would like to thank Dr. Aswin Sai Narain Seshasayee for his inputs in RNA-seq and constructive suggestions in the manuscript. We thank Edward Baidoo (Biochemist Research Scientist, Lawrence Berkley National Laboratory) for his valuable suggestions in metabolomics. We thank Colton Lloyd (Systems Biology Research Group, UCSD) for his inputs in ME-model simulations. We acknowledge Genotypic Technologies, Bangalore for library preparation and RNA sequencing. We thank Dr. Mayuri Gandhi (Research Scientist, SAIF, IIT Bombay) for providing the LCMS facility. We thank Prof. Pradeepkumar P. I. (IIT Bombay) for providing RT-PCR facility and Prof. Sarika Mehra (IIT Bombay) for providing vacuum concentrator for our use.

M.S.I acknowledges Department of Biotechnology (DBT), Government of India for his fellowship (DBT/IIT-P/323). A.P. acknowledges Department of Science and Technology INSPIRE (DST-INSPIRE), Government of India for her fellowship (IF140914).

REFERENCES

1. G. W. Li, D. Burkhardt, C. Gross, J. S. Weissman, Quantifying absolute protein synthesis rates reveals principles underlying allocation of cellular resources. *Cell* **157**, 624–635 (2014).

2. J. B. Russell, G. M. Cook, Energetics of bacterial growth balance of anabolic and catabolic reactions. *Microbiol. Rev.* **59**, 1–15 (1995).

3. K. Peebo, *et al.*, Proteome reallocation in Escherichia coli with increasing specific growth rate. *Mol. Biosyst.* **11**, 1184–1193 (2015).

4. M. Basan, *et al.*, Overflow metabolism in Escherichia coli results from efficient proteome allocation. *Nature* (2015) https:/doi.org/10.1038/nature15765.

5. S. Klumpp, Z. Zhang, T. Hwa, Growth Rate-Dependent Global Effects on Gene Expression in Bacteria. *Cell* **139 (7)**, 1366–1375 (2009).

6. S. Berthoumieux, *et al.*, Shared control of gene expression in bacteria by transcription factors and global physiology of the cell. *Mol. Syst. Biol.* **9**, 634 (2013).

7. A. Martínez-Antonio, J. Collado-Vides, Identifying global regulators in transcriptional regulatory networks in bacteria. *Curr. Opin. Microbiol.* **6 (5)**, 482–489 (2003).

8. D. C. Grainger, H. Aiba, D. Hurd, D. F. Browning, S. J. W. Busby, Transcription factor distribution in Escherichia coli: Studies with FNR protein. *Nucleic Acids Res.* **35**, 269–278 (2007).

9. Y. Kang, K. D. Weber, Y. Qiu, P. J. Kiley, F. R. Blattner, Genome-Wide Expression Analysis Indicates that FNR of. *J. Bacteriol.* **187**, 1135–1160 (2005).

10. K. S. Myers, *et al.*, Genome-scale Analysis of Escherichia coli FNR Reveals Complex Features of Transcription Factor Binding. *PLoS Genet.* **9**, 11–13 (2013).

11. S. Federowicz, *et al.*, Determining the Control Circuitry of Redox Metabolism at the Genome-Scale. *PLoS Genet.* **10 (4)**, e1004264 (2014).

12. D. M. Park, M. S. Akhtar, A. Z. Ansari, R. Landick, P. J. Kiley, The bacterial response regulator ArcA uses a diverse binding site architecture to regulate carbon oxidation globally. *PLoS Genet.* **9**, e1003839 (2013).

13. C. Constantinidou, *et al.*, A reassessment of the FNR regulon and transcriptomic analysis of the effects of nitrate, nitrite, NarXL, and NarQP as Escherichia coli K12 adapts from aerobic to anaerobic growth. *J. Biol. Chem.* **281**, 4802–15 (2006).

14. J. Zhu, S. Shalel-Levanon, G. Bennett, K. Y. San, Effect of the global redox sensing/regulation networks on Escherichia coli and metabolic flux distribution based on C-13 labeling experiments. *Metab. Eng.* **8**, 619–627 (2006).

15. N. Khoroshilova, C. Popescu, E. Münck, H. Beinert, P. J. Kiley, Iron-sulfur cluster disassembly in the FNR protein of Escherichia coli by O2: [4Fe-4S] to [2Fe-2S] conversion with loss of biological activity. *Proc. Natl. Acad. Sci. U. S. A.* **94**, 6087–6092 (1997).

16. M. W. Covert, E. M. Knight, J. L. Reed, M. J. Herrgard, B. O. Palsson, Integrating high-throughput and computational data elucidates bacterial networks. *Nature* **429**, 92–96 (2004).

17. C. L. Barrett, C. D. Herring, J. L. Reed, B. O. Palsson, The global transcriptional regulatory network for metabolism in Escherichia coli exhibits few dominant functional states. *Proc. Natl. Acad. Sci. U. S. A.* **102**, 19103–19108 (2005).

18. A. Perrenoud, U. Sauer, Impact of global transcriptional regulation by ArcA, ArcB, Cra, Crp, Cya, Fnr, and Mlc on glucose catabolism in Escherichia coli. *J. Bacteriol.* **187**, 3171–3179 (2005).

19. S. Alexeeva, K. J. Hellingwerf, M. J. Teixeira de Mattos, Requirement of ArcA for

redox regulation in Escherichia coli under microaerobic but not anaerobic or aerobic conditions. *J Bacteriol* **185**, 204–209 (2003).

20. E. W. Trotter, *et al.*, Reprogramming of escherichia coli K-12 metabolism during the initial phase of transition from an anaerobic to a micro-aerobic environment. *PLoS One* **6**, 1–7 (2011).

21. A. I. Prieto, *et al.*, Genomic analysis of DNA binding and gene regulation by homologous nucleoid-associated proteins IHF and HU in Escherichia coli K12. *Nucleic Acids Res.* **40**, 3524–3537 (2012).

22. S. M. Arfin, *et al.*, Global gene expression profiling in Escherichia coli K12: The effects of integration host factor. *J. Biol. Chem.* **275**, 29672–29684 (2000).

23. B. R. B. Haverkorn van Rijsewijk, A. Nanchen, S. Nallet, R. J. Kleijn, U. Sauer, Large-scale 13C-flux analysis reveals distinct transcriptional control of respiratory and fermentative metabolism in Escherichia coli. *Mol. Syst. Biol.* **7**, 477–477 (2014).

24. H. Bi, C. Zhang, Integration host factor is required for the induction of acid resistance in Escherichia coli. *Curr. Microbiol.* **69**, 218–224 (2014).

25. I. Aviv, H. Giladi, G. Schreiber, Expression of the genes coding for the Escherichia coli integration hohst factor are controlled by growth phase, rpoS, ppGpp and by autoregulation. *Mol. Microbiol.* **14**, 1021–1031 (1994).

26. L. M. D. Bernardo, L. U. M. Johansson, D. Solera, E. Skärfstad, V. Shingler, The guanosine tetraphosphate (ppGpp) alarmone, DksA and promoter affinity for RNA polymerase in regulation of σ54-dependent transcription. *Mol. Microbiol.* **60**, 749–764 (2006).

27. M. Scott, C. W. Gunderson, E. M. Mateescu, Z. Zhang, T. Hwa, Interdependence of Cell Growth. *Science (80-.).* **330 (6007)**, 1099–1102 (2010).

28. M. Zhu, X. Dai, Growth suppression by altered (p)ppGpp levels results from non-

optimal resource allocation in Escherichia coli. *Nucleic Acids Res.* **47**, 4684–4693 (2019).

29. C. You, *et al.*, Coordination of bacterial proteome with metabolism by cyclic AMP signalling. *Nature* **500**, 301–306 (2013).

30. S. Hui, *et al.*, Quantitative proteomic analysis reveals a simple strategy of global resource allocation in bacteria. *Mol. Syst. Biol.* **11**, e784–e784 (2015).

31. L. Reitzer, Nitrogen Assimilation and Global Regulation in Escherichia coli . *Annu. Rev. Microbiol.* **57**, 155–176 (2003).

32. F. C. Neidhardt, J. L. Ingraham, M. Schaechter, Physiology of the bacterial cell — A molecular approach. *Trends Genet.* **7 (10)**, 341 (1991).

33. M. K. Chattopadhyay, C. W. Tabor, H. Tabor, Polyamines are not required for aerobic growth of Escherichia coli: Preparation of a strain with deletions in all of the genes for polyamine biosynthesis. *J. Bacteriol.* **191**, 5549–5552 (2009).

34. W. C. Van Heeswijk, *et al.*, An alternative P(II) protein in the regulation of glutamine synthetase in Escherichia coli. *Mol. Microbiol.* **21**, 133–146 (1996).

35. H. Nikaido, Molecular Basis of Bacterial Outer Membrane Permeability Revisited. *Microbiol. Mol. Biol. Rev.* **67**, 29–47 (1996).

36. F. Wessely, *et al.*, Optimal regulatory strategies for metabolic pathways in Escherichia coli depending on protein costs. *Mol. Syst. Biol.* **7:515** (2011).

37. A. Solopova, *et al.*, Bet-hedging during bacterial diauxic shift. *Proc. Natl. Acad. Sci. U. S. A.* **111**, 7427–7432 (2014).

38. J. Utrilla, *et al.*, Global Rebalancing of Cellular Resources by Pleiotropic Point Mutations Illustrates a Multi-scale Mechanism of Adaptive Evolution. *Hepatology* **63**, 965–982 (2017).

39. C. P. Long, J. Au, N. R. Sandoval, N. A. Gebreselassie, M. R. Antoniewicz, Enzyme i facilitates reverse flux from pyruvate to phosphoenolpyruvate in Escherichia coli. *Nat. Commun.* **8**, 1–8 (2017).

40. C. D. Doucette, D. J. Schwab, N. S. Wingreen, J. D. Rabinowitz, α-ketoglutarate coordinates carbon and nitrogen utilization via Enzyme I inhibition. *Nat. Chem. Biol.* **7 (12)**, 894–901 (2011).

41. E. J. O'Brien, J. A. Lerman, R. L. Chang, D. R. Hyduke, B. Palsson, Genome-scale models of metabolism and gene expression extend and refine growth phenotype prediction. *Mol. Syst. Biol.* **9:693** (2013).

42. Minoru Kanehisa, Susumu Goto, KEGG: Kyoto Encyclopedia of Genes and Genomes. *Nucleic Acids Res.* **28 (1)**, 27–30 (2016).

43. I. M. Keseler, *et al.*, The EcoCyc database: Reflecting new knowledge about Escherichia coli K-12. *Nucleic Acids Res.* **45 (D1)**, D543–D550 (2017).

44. B. D. Bennett, *et al.*, Absolute metabolite concentrations and implied enzyme active site occupancy in Escherichia coli. *Nat. Chem. Biol.* **5 (8)**, 593–599 (2009).

45. M. Zampieri, M. Hörl, F. Hotz, N. F. Müller, U. Sauer, Regulatory mechanisms underlying coordination of amino acid and glucose catabolism in Escherichia coli. *Nat. Commun.* **10**, 3354 (2019).

46. E. Reznik, *et al.*, Genome-Scale Architecture of Small Molecule Regulatory Networks and the Fundamental Trade-Off between Regulation and Enzymatic Activity. *Cell Rep.* **20 (11)**, 2666–2677 (2017).

47. X. Dai, *et al.*, Slowdown of translational elongation in Escherichia coli under hyperosmotic stress. *MBio* **9**, 1–9 (2018).

48. H. Link, K. Kochanowski, U. Sauer, Systematic identification of allosteric protein-metabolite interactions that control enzyme activity in vivo. *Nat. Biotechnol.* **31**, 357–

361 (2013).

49. A. Pal, M. S. Iyer, S. Srinivasan, A. S. Seshasayee, K. V Venkatesh, Elucidating the regulatory role of CRP in coordinating protein biosynthesis machinery with metabolism that defines growth optimality in Escherichia coli. *bioRxiv* (2020).

50. R. Srinivasan, V. F. Scolari, M. C. Lagomarsino, A. S. N. Seshasayee, The genome-scale interplay amongst xenogene silencing, stress response and chromosome architecture in Escherichia coli. *Nucleic Acids Res.* **43 (1)**, 295–308 (2015).

51. B. K. Cho, C. L. Barrett, E. M. Knight, Y. S. Park, B. Palsson, Genome-scale reconstruction of the Lrp regulatory network in Escherichia coli. *Proc. Natl. Acad. Sci. U. S. A.* **105**, 19462–19467 (2008).

52. M. D. Bradley, M. B. Beach, A. P. J. de Koning, T. S. Pratt, R. Osuna, Effects of Fis on Escherichia coli gene expression during different growth stages. *Microbiology* **153**, 2922–2940 (2007).